Supporting Information

Conjugated Polymer Acceptors based on Fused Perylene Diimides with Twisted Backbone for Non-Fullerene Solar Cells

By Xudong Jiang, Yunhua Xu,* Xiaohui Wang, Fan Yang, Andong Zhang, Cheng Li,* Wei Ma* and Weiwei Li*

† Department of Chemistry, School of Science, Beijing Jiaotong University, Beijing 100044, P. R. China. E-mail: yhxu@bjtu.edu.cn

‡ Beijing National Laboratory for Molecular Sciences, CAS Key Laboratory of Organic Solids, Institute of Chemistry, Chinese Academy of Sciences, Beijing, 10090, China. E-mail: licheng1987@iccas.ac.cn and liweiwei@iccas.ac.cn

§ State Key Laboratory for Mechanical Behavior of Materials, Xi'an Jiaotong University, Xi'an 710049, PR China. E-mail: msewma@xjtu.edu.cn

Contents

1. Literature overview of fused PBI molecules and high performance PBI polymers

Table S1. Fused PBI molecules and high performance PBI polymers for non-fullerene solar cells reported in the literatures.

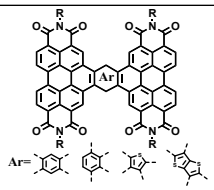 PCE 0.2%-3.9% Ref. S1.	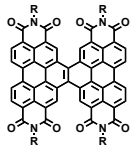 PCE 6.1% Ref. S2 and S3.	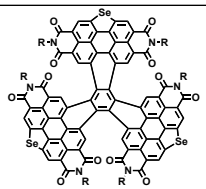 PCE 9.28% Ref. S4.
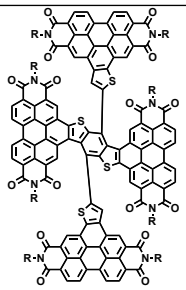 PCE 7.7% Ref. S5.	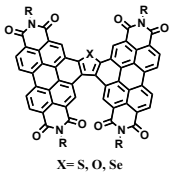 X= S, O, Se PCE 3.2%-6.7% Ref S6.	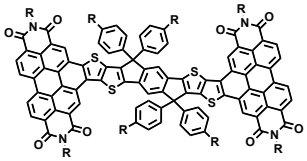 PCE 7.33% Ref S7.
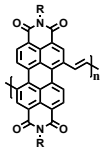 PCE 7.6% Ref. S8.	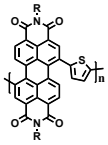 PCE 6.5% Ref. S9.	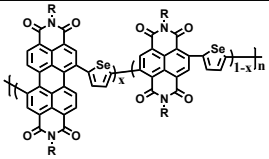 PCE 6.3% Ref. S10.
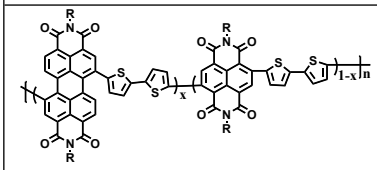 PCE 5.0% Ref. S11.		

2. Materials and measurements

All synthetic procedures were performed under argon atmosphere. Commercial chemicals were used as received. THF and toluene were distilled from sodium under an N_2 atmosphere. The compound **1**,[S12] **2**,[S12] **3**[S13] and ***trans*-PBI**[S1] were synthesized according to literature procedures. 2,5-bis(trimethylstannyl)thiophene (**M2**) were purchased from SunaTech Inc. ^{1}H-NMR and ^{13}C-NMR spectra were recorded at 500 MHz and 100 MHz on a Bruker AVANCE spectrometer with $CDCl_3$ as the solvent and tetramethylsilane (TMS) as the internal standard. Molecular weight was determined with GPC at 140 °C on a PL-GPC 220 system using a PL-GEL 10 μm MIXED-B column and *o*-DCB as the eluent against polystyrene standards. Low concentration of 0.1 mg mL^{-1} polymer in *o*-DCB was applied to reduce aggregation. TGA measurement was performed on a Perkin-Elmer TGA-7 apparatus. Differential scanning

calorimetry (DSC) was performed on a TA instruments calorimeter (Perkin Elmer Corp DSC8000) at a heating rate of 10 ºC min^{-1}. Optical absorption spectra were recorded on a JASCO V-570 spectrometer with a slit width of 2.0 nm and a scan speed of 1000 nm min^{-1}. Cyclic voltammetry was performed under an inert atmosphere at a scan rate of 0.1 V s^{-1} and 1 M tetrabutylammonium hexafluorophosphate in CH_2Cl_2 as the electrolyte, and an Ag/AgCl as a reference electrode. The counter and reference electrodes were a Pt wire and Ag/AgCl, respectively.

The organic field-effect transistors were fabricated on a commercial $Si/SiO_2/Au$ substrate purchased from First MEMS Co. Ltd. A heavily N-doped Si wafer with a SiO_2 layer of 300 nm served as the gate electrode and dielectric layer, respectively. The Ti (2 nm)/Au (28 nm) source−drain electrodes were sputtered and patterned by a lift-off technique. Before deposition of the organic semiconductor, the gate dielectrics were treated with octadecyltrichlorosilane (OTS) in a vacuum oven at a temperature of 120 °C, forming an OTS self-assembled monolayers. The treated substrates were rinsed successively with hexane, chloroform, and isopropyl alcohol. Polymer thin films were spin coated on the substrate from solution with a thickness of around 30 – 50 nm. The devices were thermally annealed at 90 °C in air for 10 min, cooled down and then moved into a glovebox filled with N_2. The devices were measured on an Keithley 4200 SCS semiconductor parameter analyzer at room temperature. The mobilities were calculated from the saturation region with the following equation: $I_{DS} = (W/2L)C_i\mu(V_G-V_T)^2$, where I_{SD} is the drain–source current, W is the channel width (1400 μm), L is the channel length (50 μm), μ is the field-effect mobility, C_i is the capacitance per unit area of the gate dielectric layer, and V_G and V_T are the gate voltage and threshold voltage, respectively. This equation defines the important characteristics of electron mobility (μ), on/off ratio (I_{on}/I_{off}), and threshold voltage (V_T), which could be deduced by the equation from the plot of current–voltage.

Photovoltaic devices with inverted configuration were made by spin-coating a ZnO sol-gel at 4000 rpm for 60 s onto pre-cleaned, patterned ITO substrates. The photoactive layer was deposited by spin coating a chlorobenzene solution containing the polymer PBDB-T and the acceptors and the appropriate amount of DIO as processing additive. MoO_3 (10 nm) and Ag (100 nm) were deposited by vacuum evaporation at ca. 4×10^{-5} Pa as the back electrode.

The active area of the cells was 0.04 cm^2. The *J-V* characteristics were measured by a Keithley 2400 source meter unit under AM1.5G spectrum from a solar simulator (Enlitech model SS-F5-3A). Solar simulator illumination intensity was determined at 100 mW cm^{-2} using a monocrystal silicon reference cell with KG5 filter. Short circuit currents under

AM1.5G conditions were estimated from the spectral response and convolution with the solar spectrum. The external quantum efficiency was measured by a Solar Cell Spectral Response Measurement System QE-R3011 (Enli Technology Co., Ltd.). The thickness of the active layers in the photovoltaic devices was measured on a Veeco Dektak XT profilometer.

Atomic force microscopy (AFM) images were recorded using a Digital Instruments Nano scope IIIa multimode atomic force microscope in tapping mode under ambient conditions. GIWAXS measurements were performed at beamline 7.3.3 at the Advanced Light Source. Samples were prepared on Si substrates using blend solutions identical to those used in devices.[S14] The 10 keV X-ray beam was incident at a grazing angle of 0.13º - 0.17º, which maximized the scattering intensity from the samples. The scattered X-rays were detected using a Dectris Pilatus 2M photon counting detector. All film samples were prepared by spin-coating solutions on Si/PEDOT:PSS substrates. The trace amount of DIO was removed under high vacuum before measurement.

R-SoXS transmission measurements were performed at beamline 11.0.1.2[S15] at the Advanced Light Source (ALS). Samples for R-SoXS measurements were prepared on a PEDOT:PSS modified Si substrate under the same conditions as those used for device fabrication, and then transferred by floating in water to a 1.5 mm × 1.5 mm, 100 nm thick Si3N4 membrane supported by a 5 mm × 5 mm, 200 μm thick Si frame (Norcada Inc.). 2-D scattering patterns were collected on an in-vacuum CCD camera (Princeton Instrument PI-MTE). The sample detector distance was calibrated from diffraction peaks of a triblock copolymer poly(isoprene-*b*-styrene-*b*-2-vinyl pyridine), which has a known spacing of 391 Å. The beam size at the sample is approximately 100 μm by 200 μm.

3. Synthesis

***cis*-PBI**. Compound **1** (200.0 mg, 0.26 mmol) and **3** (54.4 mg, 0.12 mmol) were dissolved in 5 mL toluene. Then, the reaction mixture was flushed with argon for 15 min. $Pd_2(dba)_3$ (11.8 mg, 0.013 mmol) and PPh_3 (13.5 mg, 0.052 mmol) were added, and the reaction mixture was stirred at 110 °C for 12 h. After removal of the solvent, the residue was purified by silica gel chromatography (dichloromethane: petroether = 1:1) to give a purple crude product (154 mg). This purple crude product was than dissolved in 500 ml toluene. After adding 5 mg I_2, this solution was subsequently exposed to sunlight at room temperature for 3 h. After removal of the solvent, the residue was purified by silica gel chromatography

(dichloromethane: petroether =1:1) to afford ***cis*-PBI** as an orange solid (95.2 mg, 53.3%). ^{1}HNMR (500MHz, 373 K, $CDCl_2CD\ Cl_2$): δ 9.83 (s, 2H), 9.59 (s, 2H), 9.50-9.46 (t, 4H), 9.21-9.20 (d, 2H), 9.17-9.15 (d, 2H), 5.44-5.38 (m, 2H), 4.94 (br, 2H), 2.47-2.40(m, 4H), 2.14-2.08 (m, 4H), 1.84 (br, 8H), 1.47-1.16 (m, 48H), 1.16-0.93 (m, 18H), 0.77 (m, 6H). MS (MALDI-TOF): m/z [M^-] = 1529.7 (calcd for $C_{98}H_{104}N_4O_8S_2$: 1529.7). HRMS (MALDI-TOF): m/z calcd for $C_{98}H_{104}N_4O_8S_2$ $[M]^-$: 1528.7301, found 1528.7299.

The compound **4** was prepared by using the same procedures as ***cis*-PBI** and used directly for the next bromination step without any further purification.

The monomer **M1**. A mixture of **4** (100 mg, 0.045 mmol) and bromine (2.5 ml) in 60 mL concentrated sulfuric acid was stirred at 35 °C in a round-bottom flask for 3 days. The mixture was poured into saturated sodium sulfite solution and the precipitate was collected by vacuum filtration, washed with water and methanol, dried, and purified by column chromatography on silica gel, eluted with petroleum ether/CH_2Cl_2 (1:1 v/v) to afford **M1** as an orange solid (61.5 mg, 57.4%). The monomer M1 contains two isomers that are impossible to be separated by column chromatography, so they are directly used for polymerization. ^{1}H NMR (500 MHz, 373 K, $CDCl_2CDCl_2$): δ 10.91-10.85 (m, 2H), 9.88-9.86 (d, 2H), 9.64-9.46 (m, 4H), 9.26-9.15 (m, 2H) 5.40 (br, 2H), 4.91 (br, 2H), 2.44 (br, 4H), 2.11 (br, 4H), 1.81 (br, 8H), 1.55-1.21 (m, 144H), 0.90-0.89 (m, 24H). MS (MALDI-TOF): m/z (M^-) = 2360.2 (calcd for $C_{146}H_{198}Br_2N_4O_8S_2$: 2360.3). HRMS (MALDI-TOF): m/z calcd for $C_{146}H_{198}Br_2N_4O_8S_2$ [M^-]: 2357.3023, found 2357.3011.

***cis*-polyPBI**. To a degassed solution of the **M1** (60.00 mg, 0.025 mmol) and **M2** (10.41 mg, 0.025 mmol) in toluene (2.0 mL) tris(dibenzylideneacetene)dipalladium(0) (0.69 mg, 0.8 μmol) and triphenylphosphine (1.33 mg, 3.2 μmol) were added. The mixture was stirred at 115 °C for 12 h, after which it was precipitated in methanol and filter through a Soxhlet thimble. The polymer was extracted with acetone, hexane and then dissolved in chloroform

(50 mL), which was then precipitated into acetone. Yield: 52.2 mg (89.9%). GPC (*o*-DCB, 140 °C): M_n = 18.4 kg mol^{-1}and PDI = 1.98.

4. GPC, TGA, DSC and CV plots

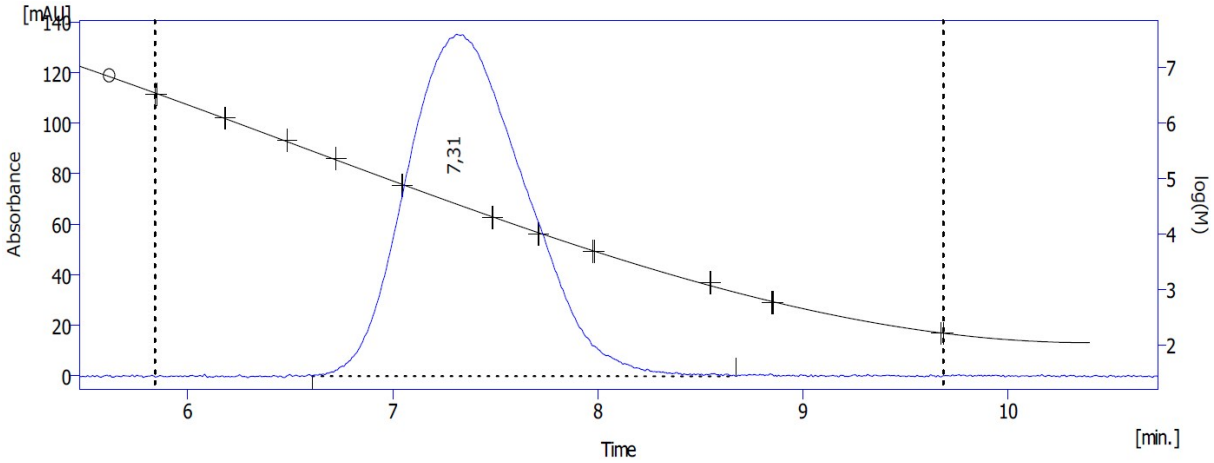

Max. RT	Start RT	End RT	Mp	Mn	Mw	Mz	Mz1	Mv	PD	Height [mAU]	Height [%]	Area [mAU.s]	Area [%]
7,313	6,61	8,67	34065	18424	36503	60606	89156	33507	1,9813	135,33	100,00	5449,69	100,00

Fig. S1 GPC recorded at 140 ºC with *o*-DCB as eluent for the polymer *cis*-polyPBI.

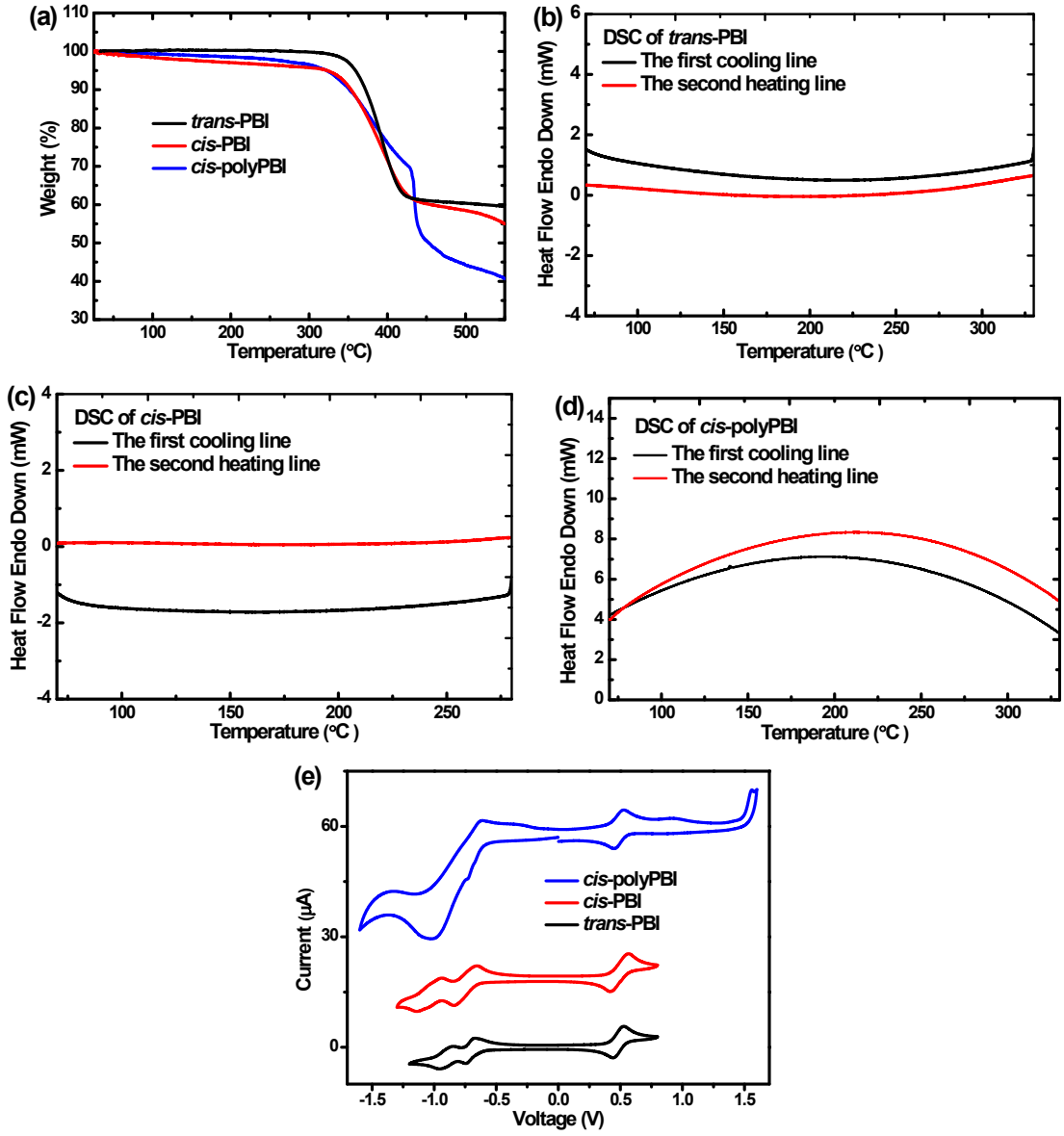

Fig. S2 (a) TGA plots of the PBI-based conjugated small molecules and polymers with a heating rate of 10 ºC/min under N_2 atmosphere. DSC heating and cooling traces of (b) *trans*-PBI, (c) *cis*-PBI and (d) *cis*-polyPBI at a scanning speed of 10 ºC/min under N_2 (endo up). (e) Cyclic voltammograms of the acceptors measured in CH_2Cl_2 at a scan rate of 0.1 V/s with ferrocene as an internal potential marker (V vs Ag/Ag^+). The plots include the signal of the ferrocene.

5. Solar cells

Table S2. Optimization of PBDB-T:*trans*-PBI inverted solar cells.

Ratio	Solvent	Thickness	J_{sc}	V_{oc}	FF	PCE

		[nm]	[mA cm^{-2}]	[V]		[%]
1:1	CB	60	0.34	1.09	0.24	0.09
1:1	CB:0.2% DIO	60	0.34	1.09	0.24	0.09
1:1	CB:0.5% DIO	60	0.42	1.10	0.29	0.13
1:1	CB:1% DIO	60	0.36	1.09	0.25	0.1
2:1	CB:0.5% DIO	60	0.17	1.03	0.31	0.05
1:1	CB:0.5% DIO	60	0.42	1.10	0.29	0.13
1:2	CB:0.5% DIO	60	0.17	1.00	0.31	0.05

Table S3. Optimization of PBDB-T:*cis*-PBI inverted solar cells.

Ratio	Solvent	Thickness [nm]	J_{sc} [mA cm^{-2}]	V_{oc} [V]	FF	PCE [%]
1:1	CB	80	11.4	0.97	0.50	5.7
1:1	CB:0.2% DIO	80	11.0	0.94	0.63	6.8
1:1	CB:0.5% DIO	80	11.9	1.00	0.64	7.6
1:1	CB:1% DIO	80	10.7	0.96	0.61	6.5
2:1	CB:0.5% DIO	80	11.4	1.02	0.57	6.6
1:1	CB:0.5% DIO	80	11.9	1.00	0.64	7.6
1:2	CB:0.5% DIO	80	10.1	1.02	0.59	6.1

Table S4. Optimization of PBDB-T:*cis*-polyPBI inverted solar cells.

Ratio	Solvent	Thickness [nm]	J_{sc} [mA cm^{-2}]	V_{oc} [V]	FF	PCE [%]
1:1	CB	80	10.2	1.0	0.62	6.2
1:1	CB:0.2% DIO	80	10.9	1.0	0.58	6.3
1:1	CB:0.5% DIO	80	10.3	1.01	0.60	6.3
1:1	CB:1% DIO	80	10.5	1.0	0.60	6.3
2:1	CB:0.5% DIO	80	11.2	1.03	0.52	6.0
1:1	CB:0.5% DIO	80	10.3	1.01	0.60	6.3

1:2	CB:0.5% DIO	80	7.9	1.01	0.61	4.8

Table S5. Photovoltaic performances of eight devices based on PBDB-T:*trans*-PBI (1:1).

Batches	J_{sc} (mA cm^{-2})	V_{oc} (V)	FF	PCE (%)
1	0.42	1.10	0.29	0.13
1	0.40	1.03	0.29	0.12
2	0.35	1.06	0.30	0.11
2	0.41	1.08	0.27	0.12
2	0.35	1.09	0.26	0.10
2	0.36	1.07	0.31	0.12
3	0.40	1.08	0.28	0.12
3	0.36	1.09	0.26	0.10

Table S6. Photovoltaic performances of eight devices based on PBDB-T:*cis*-PBI (1:1).

Batches	J_{sc} (mA cm^{-2})	V_{oc} (V)	FF	PCE (%)
1	11.88	1.00	0.64	7.59
1	11.37	0.99	0.63	7.15
2	11.16	1.00	0.64	7.05
2	10.98	1.02	0.69	7.55
2	10.82	1.02	0.68	7.50
2	11.01	1.00	0.66	7.30
3	11.37	0.99	0.63	7.09
3	11.35	0.99	0.63	7.12

Table S7. Photovoltaic performances of eight devices based on PBDB-T:*cis*-polyPBI (1:1).

Batches	J_{sc} (mA cm^{-2})	V_{oc} (V)	FF	PCE (%)
1	10.30	1.01	0.60	6.30
1	9.61	1.00	0.64	6.13
2	10.10	1.01	0.58	5.92

2	10.30	1.01	0.58	6.01
2	10.14	1.00	0.62	6.28
2	9.76	0.98	0.64	6.12
3	10.38	1.00	0.58	5.93
3	10.15	1.00	0.60	6.09

6. Synthesis of *trans*-polyPBI and its photovoltaic performance

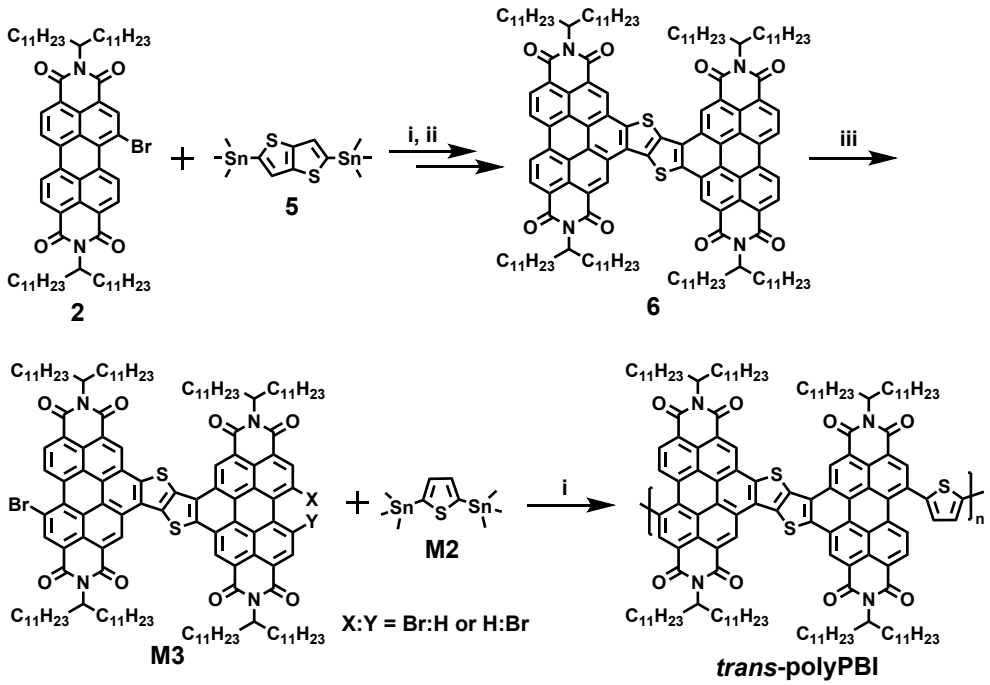

Scheme S1. Synthetic procedures of the polymer *trans*-polyPBI. (i) $Pd_2(dba)_3/PPh_3$ in toluene at 115 ºC. (ii) I_2/sunlight in toluene at 25 ºC. (iii) Br_2 in H_2SO_4 at 60 ºC.

The monomer **M3**. **M3** was synthesized following the same procedure as compound **M1** with yields of 30.9% while at 60 °C for 3 days respectively. ^{1}H NMR (500 MHz, 373 K, $CDCl_2CDCl_2$): δ 10.64 (br, 2H), 10.28 (br, 2H), 9.77 (br, 2H), 9.42 (br, 2H), 9.13-9.10 (t, 2H), 5.50 (br, 2H), 5.40 (br, 2H), 2.59 (br, 4H), 2.49 (br, 4H), 2.20 (br, 8H), 1.53-1.28 (m, 144H), 0.87-0.84 (m, 24H). MS (MALDI-TOF): m/z (M^-) = 2360.0 (calcd for $C_{146}H_{198}Br_2N_4O_8S_2$: 2360.3). HRMS (MALDI-TOF): m/z calcd for $C_{146}H_{198}Br_2N_4O_8S_2$ [M^-]: 2357.3023, found 2357.3018.

***trans*-polyPBI**. Same procedure as ***cis*-polyPBI** was used, **M2** and **M3** were used as the monomers respectively. Yield: 52.6% as a dark red solid. GPC (*o*-DCB, 140 °C): M_n = 2.3 kg mol^{-1}, M_w = 2.9 kg mol^{-1} and PDI = 1.29.

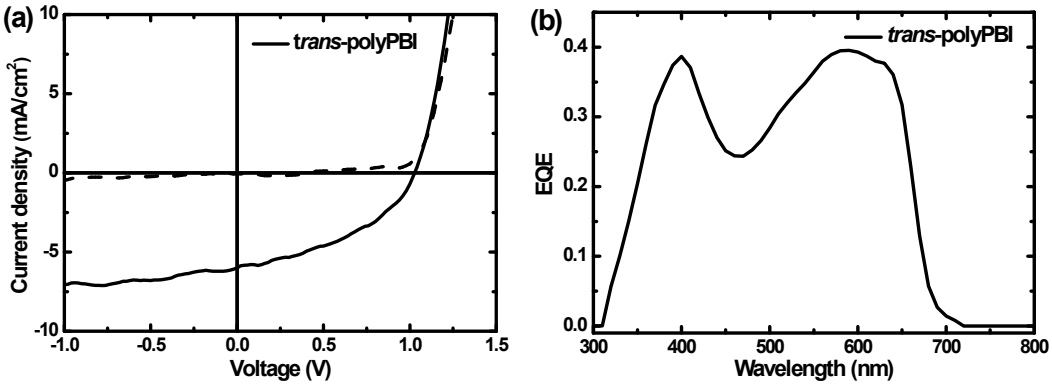

Fig. S3 (a) *J*-*V* characteristics in dark (dashed lines) and under white light illumination (solid lines) of optimized solar cells based on PBDB-T:*trans*-polyPBI (1:1) fabricated from CB/DIO (0.5%). (b) EQE of the same devices. The solar cells provided a PCE of 2.6% with J_{sc} of 6.0 mA cm^{-2}, V_{oc} of 1.02 V and FF of 0.41.

7. AFM

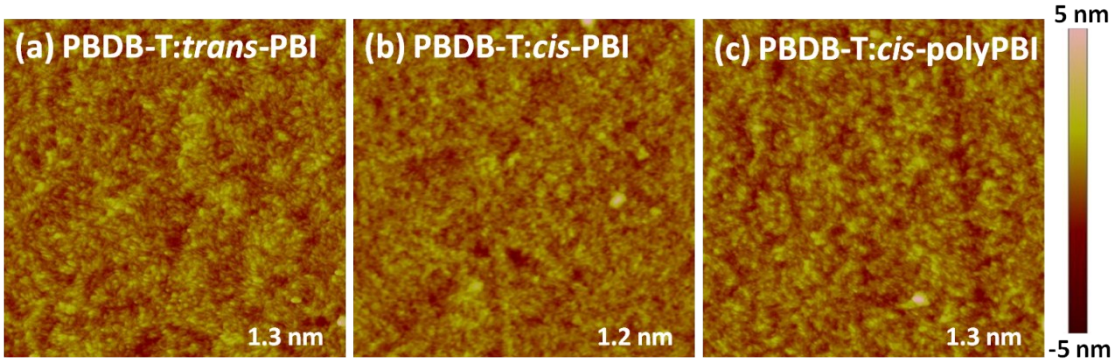

Fig. S4. AFM height image (3×3 μm^2) of the photo-active layers. The fabrication condition is referred to Table 3. The root mean square (RMS) roughness is also included.

8. NMR and MALDI-TOF

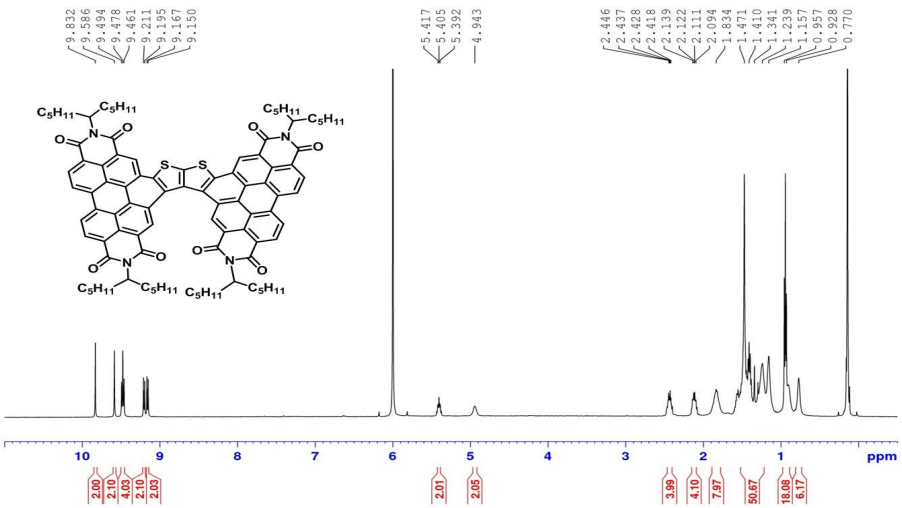

Fig. S5 ^{1}H-NMR of the molecule ***cis*-PBI** recorded at 100 ºC with 1,1,2,2-tetrachloroethane-d_2 as the solvent.

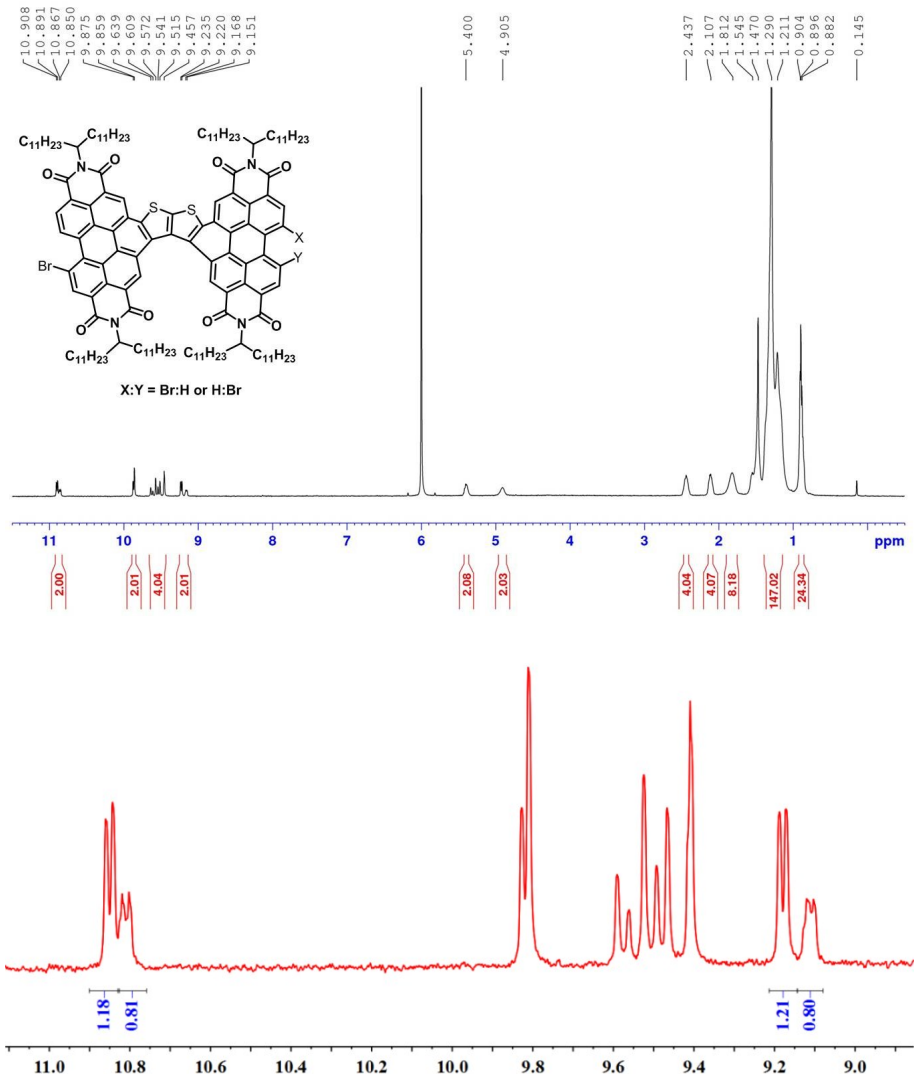

Fig. S6 ^{1}H-NMR of the monomer **M1** recorded at 100 ºC with 1,1,2,2-tetrachloroethane-d_2 as the solvent. The NMR spectrum of **M1** at aromatic region was also present, in which the ratio of isomers could be obtained with ~ 3:2.

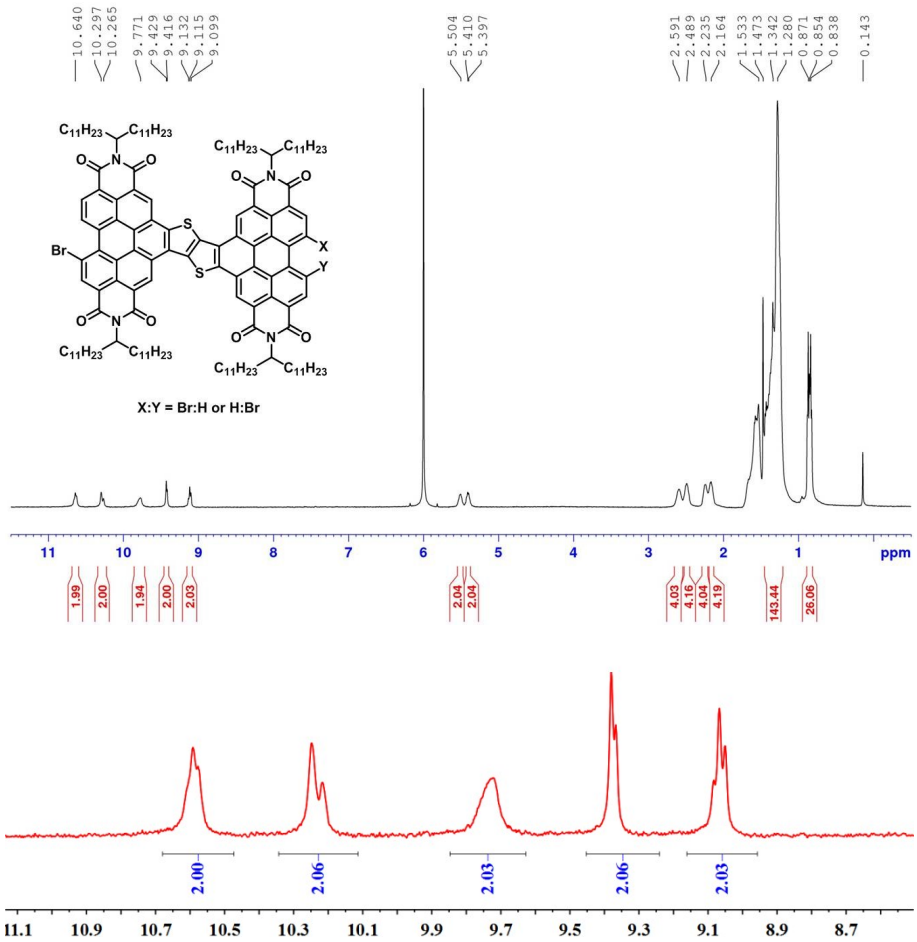

Fig. S7 ^{1}H-NMR of the monomer **M3** recorded at 100 ºC with 1,1,2,2-tetrachloroethane-d_2 as the solvent. NMR spectrum of **M3** in the aromatic region was also present, in which the splitting peaks from isomers were impossible to be distinguished.

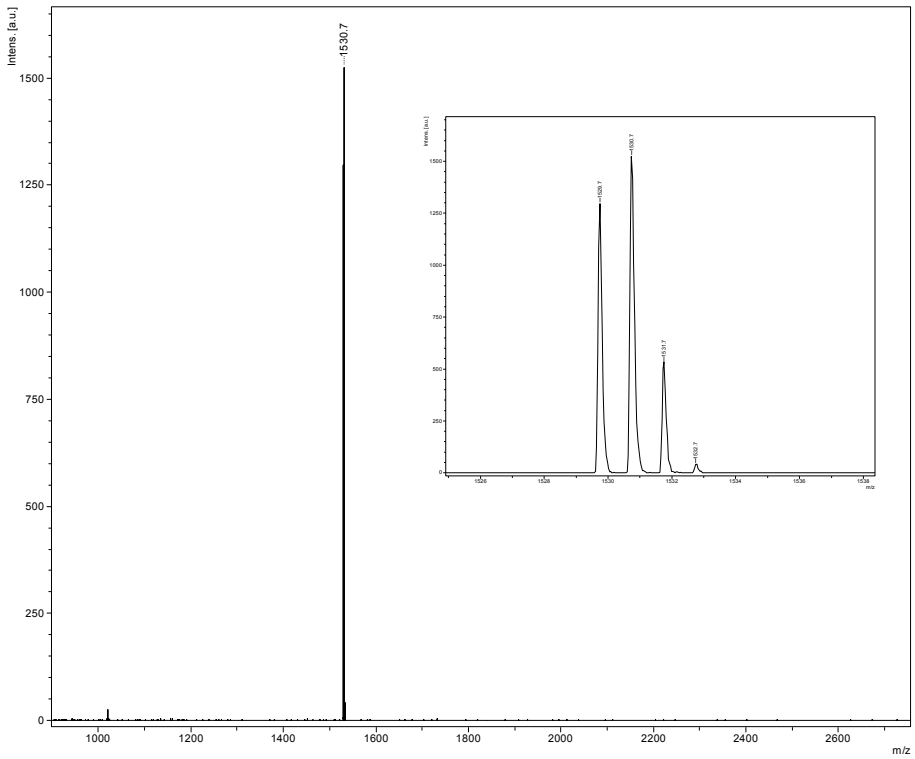

Fig. S8 MALDI-TOF spectra of ***cis*-PBI**.

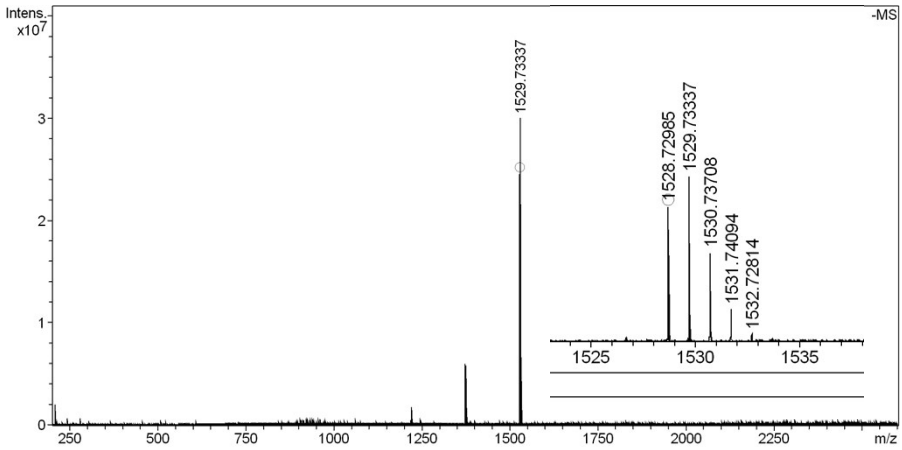

Fig. S9 High resolution MALDI-TOF spectra of ***cis*-PBI**.

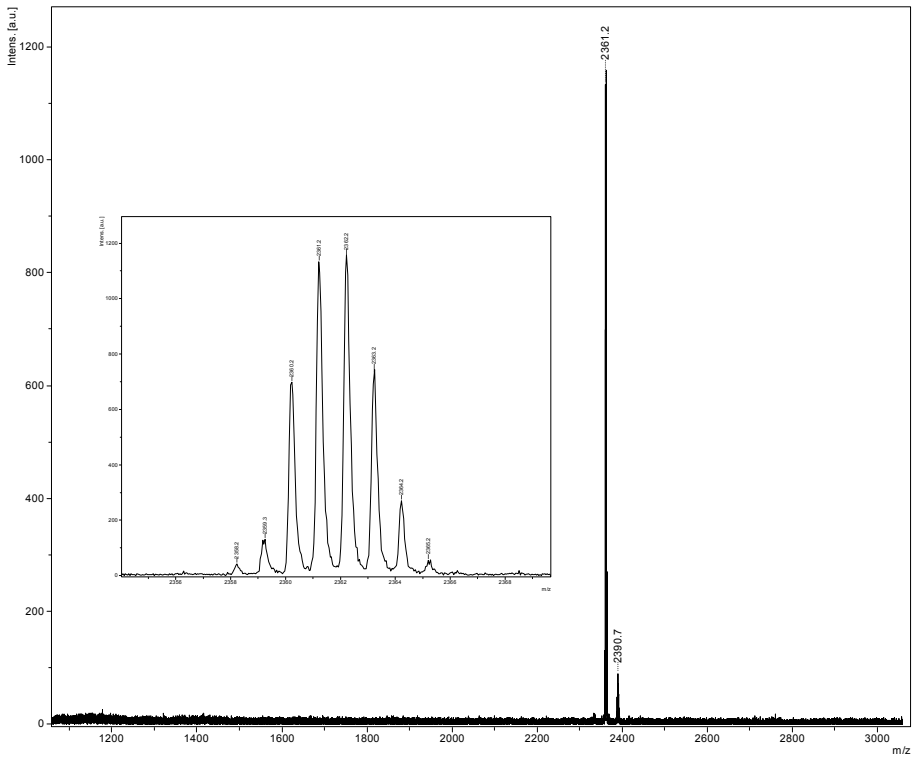

Fig. S10 MALDI-TOF spectra of the monomer **M1**.

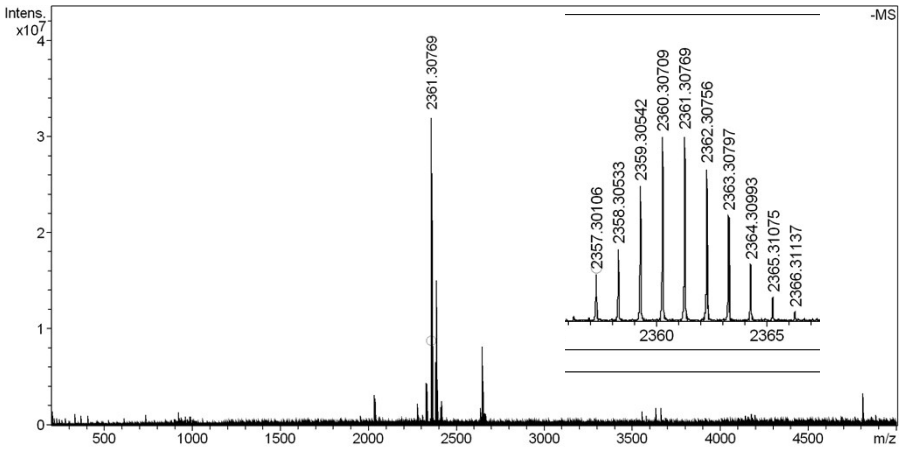

Fig. S11 High resolution MALDI-TOF spectra of the monomer **M1**.

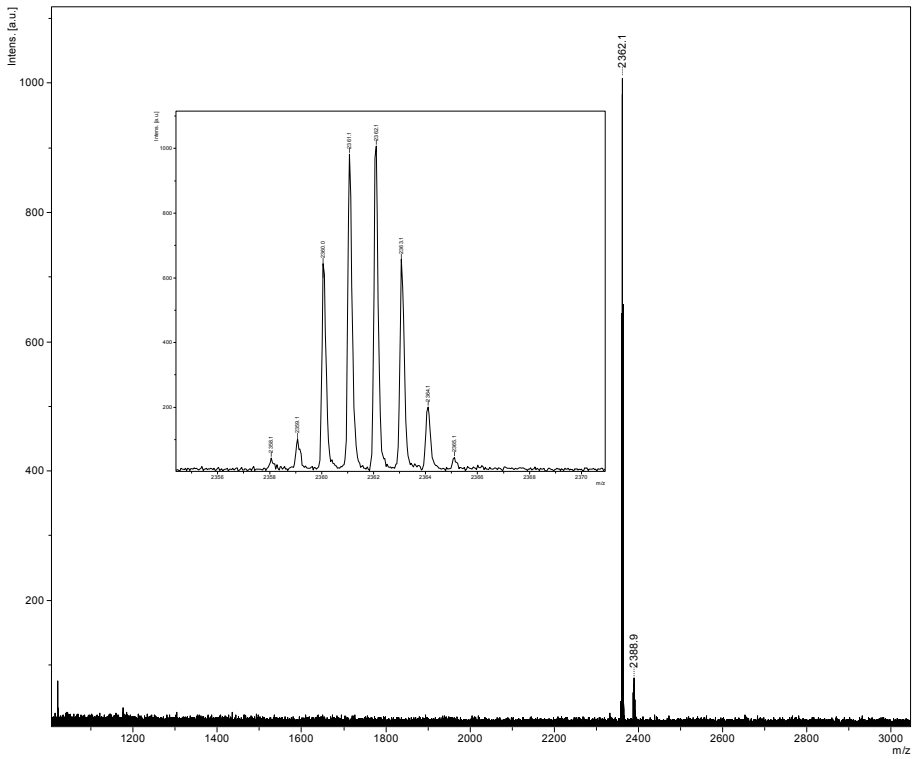

Fig. S12 MALDI-TOF spectra of the monomer **M3**.

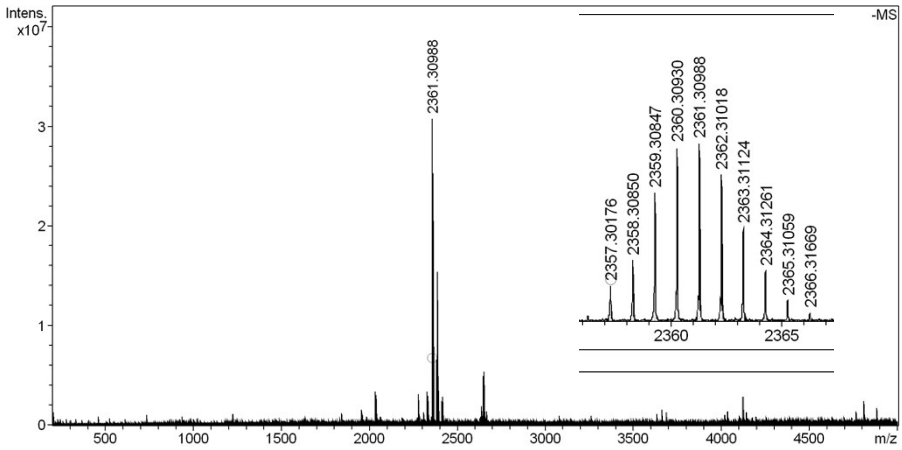

Fig. S13 High resolution MALDI-TOF spectra of the monomer **M3**.

9. References

1. P. E. Hartnett, H. S. S. R. Matte, N. D. Eastham, N. E. Jackson, Y. Wu, L. X. Chen, M. A. Ratner, R. P. H. Chang, M. C. Hersam, M. R. Wasielewski and T. J. Marks, *Chem. Sci.*, 2016, **7**, 3543-3555.
2. Y. Zhong, M. T. Trinh, R. Chen, G. E. Purdum, P. P. Khlyabich, M. Sezen, S. Oh, H. Zhu, B. Fowler, B. Zhang, W. Wang, C.-Y. Nam, M. Y. Sfeir, C. T. Black, M. L. Steigerwald, Y.-L. Loo, F. Ng, X. Y. Zhu and C. Nuckolls, *Nat. Commun.*, 2015, **6**, 8242.
3. Y. Zhong, M. T. Trinh, R. Chen, W. Wang, P. P. Khlyabich, B. Kumar, Q. Xu, C.-Y. Nam, M. Y. Sfeir, C. Black, M. L. Steigerwald, Y.-L. Loo, S. Xiao, F. Ng, X. Y. Zhu and C. Nuckolls, *J. Am. Chem. Soc.*, 2014, **136**, 15215-15221.

4. D. Meng, H. Fu, C. Xiao, X. Meng, T. Winands, W. Ma, W. Wei, B. Fan, L. Huo, N. L. Doltsinis, Y. Li, Y. Sun and Z. Wang, *J. Am. Chem. Soc.*, 2016, **138**, 10184-10190.
5. Q. Wu, D. Zhao, J. Yang, V. Sharapov, Z. Cai, L. Li, N. Zhang, A. Neshchadin, W. Chen and L. Yu, *Chem. Mater.*, 2017, **29**, 1127-1133.
6. H. Zhong, C.-H. Wu, C.-Z. Li, J. Carpenter, C.-C. Chueh, J.-Y. Chen, H. Ade and A. K. Y. Jen, *Adv. Mater.*, 2016, **28**, 951-958.
7. S. Li, W. Liu, C.-Z. Li, T.-K. Lau, X. Lu, M. Shi and H. Chen, *J. Mater. Chem. A*, 2016, **4**, 14983-14987.
8. Y. Guo, Y. Li, O. Awartani, J. Zhao, H. Han, H. Ade, D. Zhao and H. Yan, *Adv. Mater.*, 2016, 8483-8489.
9. S. Li, H. Zhang, W. Zhao, L. Ye, H. Yao, B. Yang, S. Zhang and J. Hou, *Adv. Energy Mater.*, 2016, **6**, 1501991.
10. Y.-J. Hwang, T. Earmme, B. A. E. Courtright, F. N. Eberle and S. A. Jenekhe, *J. Am. Chem. Soc.*, 2015, **137**, 4424-4434.
11. S. Sharma, N. B. Kolhe, V. Gupta, V. Bharti, A. Sharma, R. Datt, S. Chand and S. K. Asha, *Macromolecules*, 2016, **49**, 8113-8125.
12. W. Jiang, L. Ye, X. Li, C. Xiao, F. Tan, W. Zhao, J. Hou and Z. Wang, *Chem. Commun.*, 2014, **50**, 1024-1026.
13. M. Heeney, C. Bailey, K. Genevicius, M. Shkunov, D. Sparrowe, S. Tierney and I. McCulloch, *J. Am. Chem. Soc.*, 2005, **127**, 1078-1079.
14. H. Alexander, B. Wim, G. James, S. Eric, G. Eliot, K. Rick, M. Alastair, C. Matthew, R. Bruce and P. Howard, *Journal of Physics: Conference Series*, 2010, **247**, 012007.
15. E. Gann, A. T. Young, B. A. Collins, H. Yan, J. Nasiatka, H. A. Padmore, H. Ade, A. Hexemer and C. Wang, *Rev. Sci. Instrum.*, 2012, **83**, 045110.